Modeling Experimental Oscillations in Liquid Membranes with Delay Equations

J. Srividhya and M. S. Gopinathan*

Department of Chemistry, Indian Institute of Technology, Chennai-600036, India

Received: May 16, 2002; In Final Form: October 11, 2002

The oil/water interface has been of great importance in understanding the dynamics of oscillatory interfacial mass transfer phenomenon and other bio-oscillations in excitable membranes. The oscillatory mass transfer across the oil/water interface generates an oscillating interfacial potential, which is measurable with suitable experimental setup. A detailed and systematic experimental study on the CTAB/picric acid system is done and a diffusion model is studied using delay-differential equations. It is found that a two-variable model with delay in one of the variables is able to explain the observed phenomenon satisfactorily.

Introduction

Bio-oscillation or biorhythm is one of the most important properties of living organisms. In recent years, there has been an increased interest in the study of the electrical phenomena associated with excitation of membranes and oscillation of membrane potentials.[1,2] Liquid membranes are simpler systems to study the oscillatory phenomena and understand the dynamics. A liquid membrane, which is a surfactant monolayer at an oil/water interface, can exhibit interfacial potential oscillations, during which there is a transfer of surfactants from the aqueous phase to the oil phase. The phenomenon was first observed by Dupeyrat and Nakache.[3] Yoshikawa and co-workers[4] developed experiments to measure the oscillatory potential and proposed theoretical models[5,6] to explain the observed phenomena. Miyamura and co-workers[7] reported a new setup for the same system, which was easily reproducible. We have carried out experiments in a setup based on the one given by Miyamura and co-workers, but with some modifications. We observe highly reproducible oscillations in the interfacial potential with amplitude in the range 50−100 mV and frequency in the range 0.04−0.16 Hz. We also report modeling studies done using delay differential equations, with appropriate parameters derived from the experiments and literature.

Experimental Setup

The oil/water interface was constructed as follows (see Figure 1).

1. A 7.5 mL aliquot of nitrobenzene solution containing 1 mM picric acid was taken in a beaker of 5 cm i.d. (inner diameter) to form organic phase A.

2. A hollow glass tube of 1 cm i.d. was immersed in the center of the nitrobenzene solution such that 5 mm of the glass tube is inside the organic phase. The lower end of the hollow glass tube is designed to have a V-shaped deformation of 3 mm in height.

3. A 15 mL aliquot of 0.1 M D-glucose solution was then added into the beaker carefully outside the hollow tube, thus forming the aqueous phase B as in Figure 1.

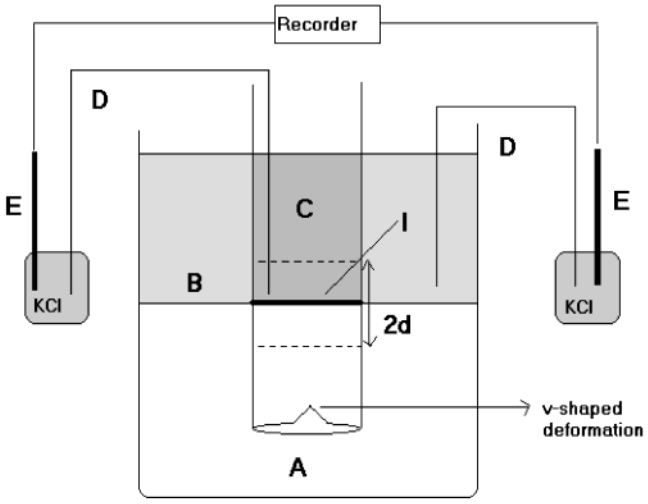

Figure 1. Experimental setup for measuring the oscillating interfacial potential. Key: (A) picric acid in nitrobenzene; (B) glucose; (C) CTAB + *n*-butanol; (I) interface; (D) salt bridge; (E) Ag−AgCl electrode.

4. A 2.3 mL aliquot of a mixture of aqueous cetyltrimethylammonium bromide (CTAB) solution (with various concentrations as described later) and 0.5 M *n*-butanol was added very slowly using a micropipet, to the inner tube to form another aqueous phase C as in Figure 1. At this height of immersion of the hollow tube (5 mm), the electrical potential generated at the interface started oscillating spontaneously. Oscillations do not occur if the height of immersion is greater than 5 mm.

Potential measurement was made using two salt bridges, D in Figure 1 (tip narrowed to 2 mm), placed very near to the interfaces, with the other end in a solution of 3 M KCl, and the potential measured with two Ag−AgCl reference electrodes "E". The signal collected was then sent to a computer through an A−D converter. The sampling time was maintained as 0.14 s. The water/nitrobenzene/water system constructed by us differed from the one given by Yoshihisa and co-workers[8] in that a simple glass tube with a V-shaped deformation (3 mm) at the basal boundary was used by us instead of a Teflon tube with a (0.3 mm) notch. This deformation is helpful in sustaining the oscillations for a longer time (over 30 min) and also gives rise to some complex behavior of the potential, which we have

* Corresponding author. E-mail address: gopi@iitm.ac.in. Fax: +91-44-22578241. Phone: +91-44-22578246.

10.1021/jp021240z CCC: $25.00
Published on Web 01/11/2003

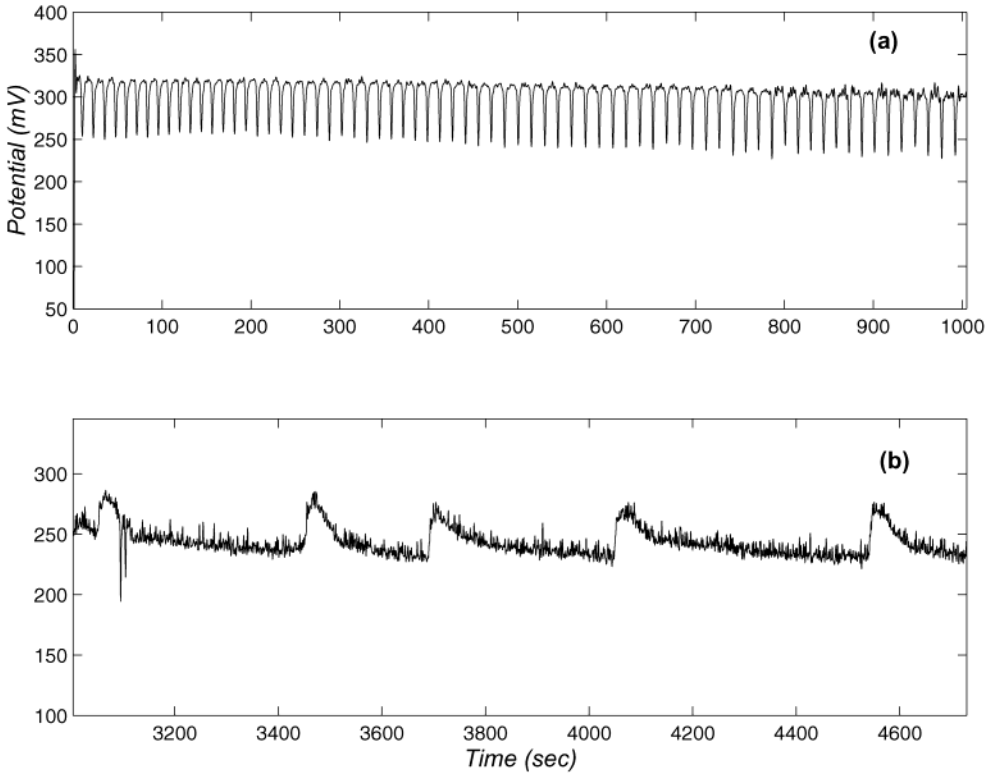

Figure 2. Experimental time series for 6 mM CTAB with picric acid: (a) high-frequency oscillations; (b) low-frequency oscillations.

observed for the first time at the later stages of the experiment before the cessation of the oscillations.

The measured time series of the interfacial potential ($E(t)$) for one particular concentration of CTAB and picric acid is shown in Figure 2a. Figure 2b shows the low-frequency oscillations observed at the final stages of the experiment. It is clearly seen that regular oscillations of frequency 0.04−0.16 Hz with amplitude 70−80 mV is sustained for over 30 min. This behavior is seen for various concentrations of CTAB and picric acid. There exists a threshold concentration of CTAB (3 mM) below which there is no sustained oscillation. The concentration of picric acid on the other hand has an upper limit of 1.2 mM above which no sustained oscillation takes place. We observe period-1 oscillations at the concentrations of CTAB and picric acid used by us, in contrast to ref 9 who have reported multiple periodicities below 0.8 mM picric acid. The reconstructed attractors of our time series for picric acid concentrations of 1 and 0.4 mM are shown in Figure 3. The attractors were reconstructed from the observed time series using the method in refs 10 and 11, and the reconstruction lag time was fixed using the method given in ref 12. The reconstructed attractors for these two concentrations look similar and clearly show that the oscillations are a single period. The finite width of the attractor is due to the noise in the measurement. The difference between our results and those of ref 9 may probably be attributed to the difference in the experimental conditions where the authors of ref 9 have carried out the experiments in a U-tube.

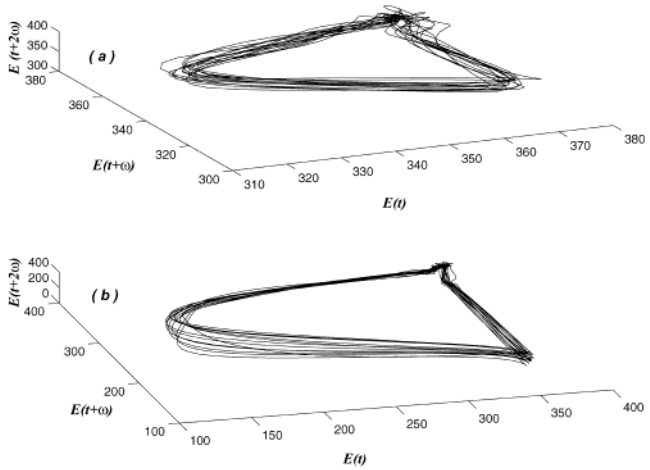

Figure 3. Reconstructed attractor from the measured time series for 5 mM CTAB with (a) 1 mM picric acid (reconstruction lag time $\omega = 8$ s) and (b) 0.4 mM picric acid (reconstruction lag time $\omega = 18$ s).

Theoretical Modeling

In this study we model only the sustained high-frequency oscillations. The model is based on the following mechanism proposed by Toko and co-workers.[5] CTAB and picric acid diffuse from the bulk to the interface. At the interface, there is an ion pair complex formation. The complex formation continues until a threshold concentration of CTAB is reached at the interface. Then the complex molecules are abruptly transferred into the organic phase. This is then followed by readsorption of CTAB and picric acid and the whole process repeats.

The mechanism we model is in principle similar to the one in the ref 5 except that we set the rate of change of CTAB concentration to be dependent on the concentration of CTAB at an earlier time (a delayed variable). This delay is introduced to take into account the finite time required for the diffusion of the molecules from the bulk to the interface.

Delay differential equations are used to model the system based on diffusion and adsorption kinetics. The following are the equations that we propose to describe the dynamics of the

system at the interface.

$$\frac{dX(t)}{dt} = \frac{D_x A}{\upsilon d}[X_b - X(t-\delta)] - kX(t)\,Y(t) + f(X) \quad (1)$$

$$\frac{dY(t)}{dt} = \frac{D_y A}{\upsilon d}[Y_b - Y(t)] - kX(t)\,Y(t) \quad (2)$$

where $f(X) = k_L[X_L - X(t)]^m$.

X and Y are the respective interfacial concentrations of CTAB and picric acid. X_b and Y_b are the respective bulk concentrations of CTAB and picric acid, d is the thickness of the interfacial sublayer in cm perpendicular to the interface, A is the area in cm^2 across which the transfer takes place, k is the rate constant of the formation of complex or the ion pair in $M^{-1}\ s^{-1}$, D_x and D_y are the diffusion coefficients of CTAB and picric acid, respectively, in $cm^2\ s^{-1}$, υ is a constant equal to 1 cm^3, and X_L is the limiting concentration or the threshold concentration of CTAB at the interface in M above which breakage of monolayer takes place. k_L is the proportionality constant for the above process, and m is the Hill's coefficient. δ is the delay in seconds.

The high-frequency oscillations that constitute a major part of the time series (over 30 min) alone is considered in modeling. The model is based on the following assumptions:

1. The bulk concentrations of CTAB and picric acid are assumed to be constant.

2. Diffusion is always associated with a finite delay in time.[13] Hence time delayed variable $X(t - \delta)$ is used in the diffusion term of the differential equation. Because both CTAB and picric acid reach the interface by diffusion, the delay δ can be taken for simplicity as the effective total delay caused due to both CTAB and picric acid. In other words, only X is treated as a delayed variable. Delay δ is taken to be the average time interval between the onset of adsorption, as indicated by the begining of the oscillatory cycle in the $E(t)$ time series, and the completion of adsorption of the monolayer, as indicated by the beginning of the decrease in maximum amplitude in the oscillatory cycle.

3. The thickness of the interfacial sublayer (d) is assumed to be constant during the high-frequency phase of the experiment.

Equations 1 and 2 are based on the adsorption kinetics for mass transfer.[14] The first term in eq 1 refers to the diffusive adsorption of the surfactant molecules (X) from the aqueous bulk, C in Figure 1, onto the interface I in Figure 1.

The second terms in eqs 1 and 2 refer to the formation of the ion pair complex. k is the rate constant of formation of the complex, which is measured from the experiment. The rate of complex formation depends on the interfacial concentrations of both CTAB and picric acid. With one of the concentrations kept constant, the reaction was assumed to be pseudo unimolecular. Then by varying the concentration of the other species, the rate constant was determined to be 110.0 $M^{-1}\ s^{-1}$. The details of the measurement of the rate constant are given in the next section.

The third term $f(X)$ in eq 1 is introduced to account for the suppression of the monolayer formation when the concentration of surfactant at the interface reaches a limiting value X_L. The value of the scaled limiting concentration was taken to be 1 in all the calculations because the limiting concentration is proportional to the bulk concentration of CTAB. The Hill's coefficient m gives the average number of CTAB molecules per binding site. The value of m is calculated as described in ref 15 from the plot of $\log(\theta/(1-\theta))$ vs [CTAB], where θ is the fraction of surface covered. The slope of the plot gives the value of m and was found to be approximately equal to 5. The details of the measurement of the Hill's coefficient are given in the next section.

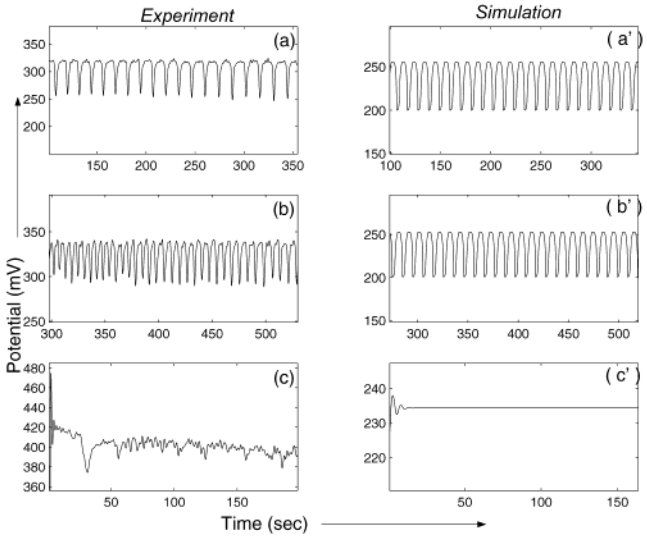

Figure 4. Comparison between simulation and experimental time series for 1 mM picric acid with (a, a′) 6 mM CTAB (b, b′) 4 mM CTAB, and (c, c′) 1 mM CTAB. The scaled delay τ used in (a′), (b′), and (c′) are 3.08, 2.9, and 1.0, respectively.

We can recast eqs 1 and 2 into dimensionless form as

$$\frac{dx}{dt'} = 1 - x(t'-\tau) - cxy + f(x) \quad (3)$$

$$\frac{dy}{dt'} = a - by - cxy \quad (4)$$

Here $x = X/X_o$, $y = Y/X_o$, $t' = t/t_o$, and $\tau = \delta/t_o$, where $t_o = d\upsilon/D_xA$, $X_o = X_b$ and $f(x) = g(1-x)^m$. With $d = 550$ Å, $\upsilon = 1\ cm^3$, $D_x = 6 \times 10^{-6}\ cm^2\ s^{-1}$, $D_y = 5 \times 10^{-6}\ cm^2\ s^{-1}$,[14] and $A = 0.785\ cm^2$, the value of t_o was found to be 1.1671 s. With the above scaling factors, $a = r(D_y/D_x)$, where $r = Y_b/X_b$ and $b = (D_y/D_x)$ and $c = kX_ot_o$, $g = k_LX_o^{m-1}t_o$.

Equations 3 and 4 were solved for various parameter values as determined from the experiment (see following section for details). Mathematica 4.0 was used to solve the delay differential equation.[16] The variable $X(t)$ from the solution was then converted to potential using the following expression based on the Guoy−Chapmann equation for interfacial potential.[14]

$$E = \frac{2k_BT}{e}\sinh^{-1}\frac{\sigma}{\sqrt{2\epsilon_w k_B T x_b/\pi}} \quad (5)$$

$\sigma = eX(t)/a_o$. E is the potential at the interface in millivolts, k_B is Boltzmann constant in cal K^{-1}, T is temperature in Kelvin, e is electronic charge in Coulombs C, ϵ_w is dielectric constant of water (78 at 25 °C), and a_o is the area occupied by one molecule, taken as $25 \times 10^{-16}\ cm^2$.[14] Figures 4 and 5 show the simulated time series and the experimental time series ($E(t)$) for various parameter values.

Measurement of Parameters from Experiment

Rate Constant. The rate constant k appearing in eqs 1 and 2 was determined as follows. The complex formed was assumed to be 1:1 and the rate of the complex formation is dependent on both CTAB and picric concentrations. But for sufficiently large bulk concentrations of picric acid (2 mM), the interfcial concentration of picric acid (Y) was found to be a constant by

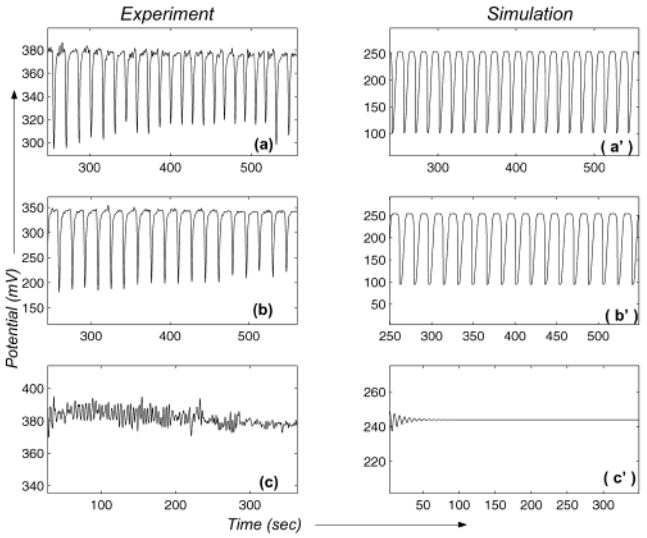

Figure 5. Comparison between simulation and experimental time series for 5 mM CTAB with (a, a′) 0.8 mM picric acid, (b, b′) 0.5 mM picric acid, and (c, c′) 2 mM picric acid. The scaled delay τ used in (a′), (b′), and (c′) are 5.0, 6.0, and 1.5, respectively.

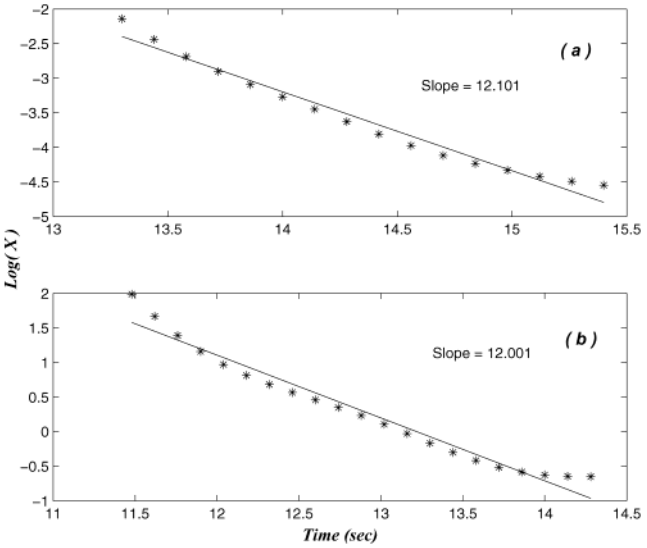

Figure 6. Determination of rate constant for complex formation. Plot of log(X) with respect to time in seconds for 2 mM picric acid with (a) 5 mM CTAB and (b) 6 mM CTAB as bulk concentrations.

the measurement of pH at the interface. Hence the rate of complex formation at this concentration of picric acid can be taken as dependent on CTAB only, i.e., pseudo-first order in CTAB concentration. For the reaction X + Y $\rightarrow$ complex, we set $dX/dt = k''X$, where $k'' = kY$.

The interfacial potential was measured with respect to time for 2 mM picric acid with 5 and 6 mM CTAB and was converted into concentration using eq 5. A plot (see Figure 6) of log(X) versus time t for different bulk concentrations of CTAB gave a straight line plot with $k'' = 12.051\ s^{-1}$ as an average. The constant Y was measured as follows. The hydrogen ion concentration in the aqueous phase very near to the interface can be considered to represent the picrate concentration (due to dissociation) at the interface, available for the complex formation. The hydrogen ion concentration was measured with a pH meter of 3 mm diameter by placing it very near to the interface and was found to be 0.9601, which corresponds to a hydrogen ion concentration of 0.1096 M and which is equal to

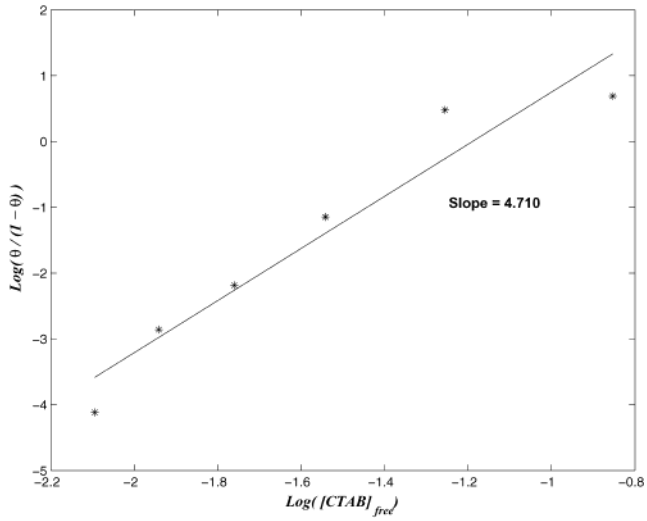

Figure 7. Determination of Hill's coefficient. Plot of log($\theta/(1-\theta)$) vs log([CTAB]$_{free}$).

Y. The pH was found to be a constant throughout the experiment.Then k was calculated to be 110.0 $M^{-1}\ s^{-1}$.

Hill's Coefficient. The interfacial potential was measured at equilibrium for different bulk concentrations of CTAB starting from 1 to 7 mM, over a plain nitrobenzene interface. The corresponding interfacial concentration at equilibrium x_{eq} was obtained using eq 5. The maximum interfacial concentration x_{max} of CTAB within the interfacial sublayer volume, for the given interfacial surface area (0.785 cm^2) was theoretically calculated by knowing the area occupied by one molecule of CTAB (25×10^{-16} cm^2) from the literature.[14] The ratio $\theta = x_{eq}/x_{max}$ is the fraction of surface covered. A plot of log($\theta/(1-\theta)$) versus log([CTAB]$_{free}$)[15] (see Figure 7) gave a straight line with slope 4.710, which is Hill's coefficient. [CTAB]$_{free}$ was calculated from the value of K_m ($=5.04 \times 10^7$ see ref 17), which is the equilibrium constant of micellization of CTAB at room temperature.

Construction of Parameter Space

Linear stability analysis for the above set of eqs 3 and 4 has been done. x^* and y^*, the steady-state concentrations, are obtained by putting $\tau = 0$ and equating the rates in eqs 3 and 4 to zero. The values of the parameters are $a = 0.833\ r$, $b = 0.83$, $c = 128.4\ X_o$, $g = 1$, and $m = 5$. It may be noted that the steady states are dependent on the value of r. For example, steady-state values were $x^* = 0.518$ and $y^* = 1.09$ when $r = 0.142$ and $x^* = 0.577$ and $y^* = 1.176$ for $r = 0.2$.

Assuming $x(t' - \tau) = x(t')e^{-\lambda\tau}$ for small values of delay, the Jacobian for the above set of differential equations (3) and (4) is as follows.

$$\begin{bmatrix} -e^{-\lambda\tau} - cy^* + f'(x^*) & -cx^* \\ -cy^* & -b - cx^* \end{bmatrix}$$

Here $f'(x^*)$ is the first derivative of $f(x)$ with respect to x in eq 3 evaluated at steady state x^*. This gives the following characteristic equation for the eigen values λ of the Jacobian:

$$\lambda^2 + \lambda[cx^* + cy^* + b - f'(x^*)] + \lambda e^{-\lambda\tau} + [b + cx^*]e^{-\lambda\tau} + cy^*b - f'(x^*)[cx^* + b] = 0 \quad (6)$$

Equation 6 is transcendental in nature and hence solved for λ numerically.

TABLE 1: Comparison between Experimental and Simulated Oscillations

CTAB with 1 mM Picric Acid					
				nature of oscillations	
conc (mM) of CTAB	conc ratio r	measd delay (s)	scaled delay τ	experiment	simulation
7.0	0.143	3.67	3.14	sustained	stable limit cycle
6.0	0.166	3.60	3.08	sustained	stable limit cycle
5.0	0.200	3.50	3.0	sustained	stable limit cycle
4.0	0.250	3.40	2.9	sustained	stable limit cycle
3.0	0.333	1.86	1.6	damped	stable focus
2.0	0.500	1.746	1.5	damped	stable focus
1.0	1.000	1.50	1.0	damped	stable focus
Picric acid (PA) with 5 mM CTAB					
				nature of oscillations	
conc (mM) of CTAB	conc ratio r	measd delay (s)	scaled delay τ	experiment	simulation
2.0	0.400	1.75	1.5	damped	stable focus
1.5	0.300	1.86	1.6	damped	stable focus
1.2	0.240	2.33	2.0	sustained	stable limit cycle
1.0	0.200	3.50	3.0	sustained	stable limit cycle
0.8	0.160	5.83	5.0	sustained	stable limit cycle
0.5	0.100	7.00	6.0	sustained	stable limit cycle
0.4	0.080	8.17	7.0	sustained	stable limit cycle

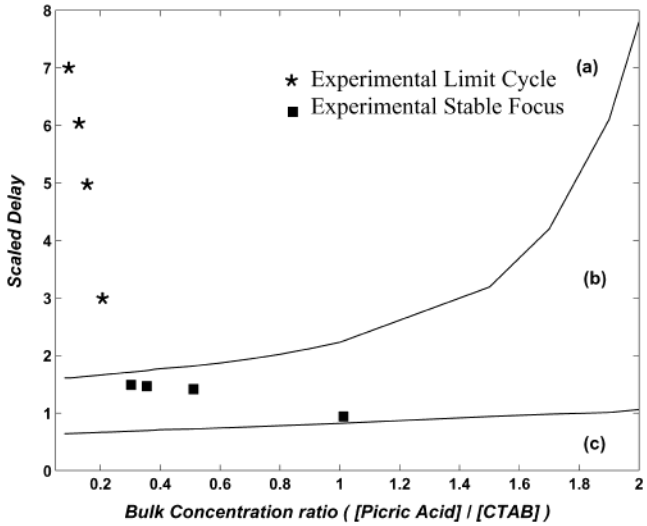

Figure 8. Parameter space diagram for varying values of delay (scaled) and bulk concentration ratio: (a) limit cycle; (b) damped oscillatory; (c) nonoscillatory.

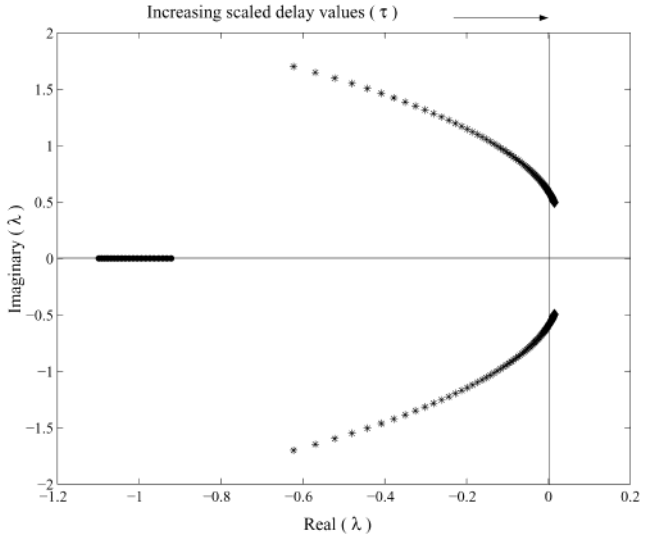

Figure 9. Variation of eigenvalues of the Jacobian with respect to the increase in scaled delay values τ.

For $\lambda = \alpha$ where $\alpha < 0$ the system is nonoscillatory, for $\lambda = \alpha + i\beta$ where $\alpha < 0$ the system is in stable focus, i.e., stable oscillatory, and for $\lambda = \alpha + i\beta$ where $\alpha > 0$ the system is in a stable limit cycle. Equation 6 is solved for various values of bulk concentration ratios r (Y_b/X_b) and delays τ. A parameter space diagram is obtained by plotting the eigenvalue λ as a function of the parameters r and τ. Experiments were carried out for different concentration values of both CTAB and picric acid. Table 1 gives the values of experimental quantities as a function of r and τ and a comparison of the nature of oscillations from experiments and simulations.

Discussion

The parameter space diagram (Figure 8) shows various regimes representing nonoscillatory, damped oscillatory, and limit cycle behaviors. The points on the diagram represent the experimental position of the system for the corresponding concentration ratio r and scaled delay value τ estimated from experiment. It can be observed from Table 1 and Figure 8 that the predicted nature of oscillatory behaviors such as damped oscillations and limit cycle ocillations agree very well with the observations.

The variation of eigenvalue λ for increasing τ values from 0 to 5 is shown in Figure 9. We see that there exists a threshold value of the delay τ for the system to exhibit limit cycle (sustained) oscillations. It is to be noted that the delay term introduces sufficient nonlinearity in the system of equations. The frequency of the oscillations plotted against the bulk concentration of picric acid, from the simulated time series also follows the same trend as observed in the experiments (Figure 10).

The close correlation between the simulation and the experiment shows that the interface mediated transport process can also be viewed as a simple dynamical process and can be explained in terms of delay differential equations without involving the interface related phenomena like Marangoni effect,[18] surface pressure−area isotherms,[19] etc. Our model seems to give an insight about the mechanism because the parameter values were actually taken from the experiments and literature.

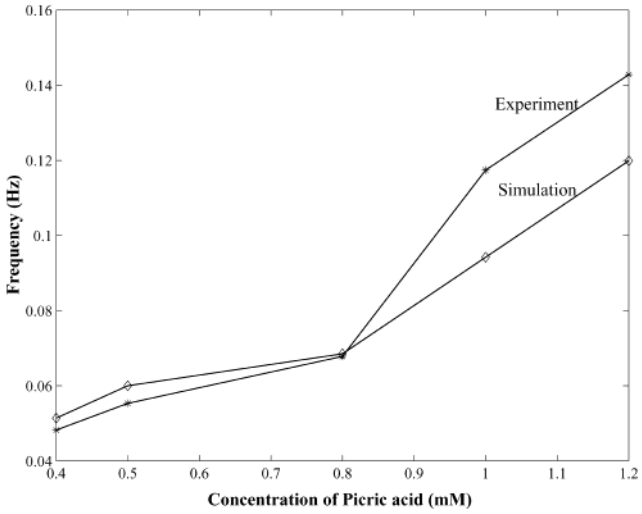

Figure 10. Comparison of frequencies from experiment and simulation for 5 mM CTAB with various concentrations of picric acid.

Conclusion

It is seen that a system of coupled two-variable delay differential equations reproduce the dynamics of the oscillatory mass transfer of the surfactant across the oil/water interface. Modeling such oscillatory systems can give an insight into the dynamics of mass transport across biological membranes. The presence of delay, which is very significant in physiological and other biological processes,[13] seems to be important even in simpler systems like the oil/water interface studied here.

Acknowledgment. This work was supported by the Center for scientific and Industrial research (CSIR-India). We sincerely thank Emeritus Prof. R. Ramaswamy, IIT-Chennai, for his valuable suggestions and help in building the apparatus for all the experiments.

References and Notes

(1) Larter, R. *Chem. Rev.* **1990**, *90*, 355−381.
(2) Kim, J. T.; Larter, R. *J. Phys. Chem.* **1991**, *95*, (20), 7948−7955.
(3) Nakache, E.; Dupeyrat, M. *J.Colloid Interface Sci.* **1983**, *94* (1) 187−200.
(4) Yoshikawa, K.; Matsubara, Y. *J. Am. Chem. Soc.* **1983**, *105*, (19), 5967−5969.
(5) Toko, K.; Yoshikawa, K.; Tsukiji, M.; Nosaka, M.; Yamafiju, K. *Biophys. Chem.* **1985**, *22*, 151−158.
(6) Yoshikawa, K.; Shoji,M.; Nakata, S.; Maeda, S.; Kawakami, H. *Langmuir* **1988**, *4*, 759−762.
(7) Miyamira, K.; Morooka, H.; Hirai, K.; Gohshi, Y. *Chem. Lett.* **1990**, 1833−1836.
(8) Yoshihisa, H.; Sutou, S.; Miyamura, K.; Gohshi, Y. *Anal. Sci.* **1998**, *14*, 133−136.
(9) Takahashi, K.;Yasukawa, H.; Sugimura, T. *Chem. Lett.* **1994**, 2085−2088.
(10) Takens, F. *Lecture Notes in Mathematics*; Springer: Berlin, 1981; No. 898, pp 366−381.
(11) Packard, N. H.; Grutchfield, J. P.; Farmer, J. D.; Shaw, R. S. *Phys. Rev. Lett.* **1980**, *45*, 712−716.
(12) Kaplan, D. T.;Glass, L. *Understanding Nonlinear Dynamics*; Springer-Verlag: NewYork, 1995.
(13) Scheper, T.; Klinkenberg, D.; Pennartz, C.; Pelt, J. *J. Neuroscience* **1999**, *19* (1), 40−47.
(14) Davies, J. T.; Rideal, E. K. *Interfacial Phenomena*; Academic Press: New York, 1961.
(15) Laidler, Keith J. *Physical Chemistry with biological applications*; The Benjamin/Cummings Publishers: 1978.
(16) Software Package NDelayDSolve.m written by Allan Hayes was used to solve the delay differential equation and is freely downloadable at the site http://www.mathsource.com/Content/Enhancements/Numerical/0209−102.
(17) Byung Hwan Lee. *J, Korean Chem, Soc*, **1994**, *38* (8), 539−546.
(18) Suzuki, H.; Tsuchiya, Y. *Physica D* **1995**, *84*, 276−279.
(19) Yoshikawa, K.; Makino, M.; Nakata, S.; Ishii, T. *Thin Solid Films* **1989**, *180*, 117−121.